

Research Article

Evaluation of Seismic Performance of Reinforced Concrete Frame Structures in the Context of Big Data

Du Guangqian ¹, Zheng Meng,² and Wang Shijie ¹

¹Urban and Rural Construction Institute, Agricultural University of Hebei, Baoding, Hebei 071001, China

²School of Mechanical Engineering, Beijing Institute of Technology, Beijing 10008, China

Correspondence should be addressed to Wang Shijie; wshj_wshj@sohu.com

Received 12 June 2018; Revised 14 August 2018; Accepted 20 August 2018; Published 8 January 2019

Academic Editor: Zhihan Lv

Copyright © 2019 Du Guangqian et al. This is an open access article distributed under the Creative Commons Attribution License, which permits unrestricted use, distribution, and reproduction in any medium, provided the original work is properly cited.

In the era of big data, the efficient use of idle data in reinforced concrete structures has become a key issue in optimizing seismic performance evaluation methods for building structures. In this paper, based on the evaluation method of structural displacement seismic performance and based on the characteristics of high scalability and high fault tolerance of the cloud platform, the open source distributed and storage features of the Hadoop architecture cloud platform are introduced as a subproject of Apache Nutch project, Hadoop cloud platform. With features such as high scalability, high fault tolerance, and flexible deployment, the storage platform is secure, stable, and reliable. From the evaluation of the seismic performance of newly-built buildings and existing damaged buildings, according to the structural strength-ductility theory of the structure, the building structure resists earthquakes with its strength and ductility and buildings are divided into four categories. Due to the influence of time or seismic damage on the structure of reinforced concrete frame structures, their material properties are often deteriorating. Using the distributed computing design concept to efficiently process big data, a dynamic evaluation model for the seismic performance of reinforced concrete frame structures is established. A project of a 10-story reinforced concrete frame structure was selected for calculation and analysis; the engineering example was used to verify the accuracy and efficiency of the model, and the seismic performance of the floor was analyzed. It can be seen that the initial stiffness index of the structure is not sensitive to the damage location of the structure. The platform based on the concept of distributed computing big data processing can effectively improve the efficiency and accuracy of the evaluation of reinforced concrete frame structures.

1. Introduction

The seismic evaluation theory for building structures with reinforced concrete structure performance is based on the investigation and statistics of a large number of seismic damage data and scientific analysis. With the advent of the era of big data, the accuracy, comprehensiveness, and efficiency of the evaluation of seismic performance have also increased. He et al. estimated the seismic performance of rural residential buildings in Guangzhou from the aspects of building structure, building age, and building fortification and put forward the countermeasures and suggestions for earthquake prevention and disaster reduction of rural

residential buildings. The flaws of the seismic evaluation theory and the seismic design theory gradually exposed. The American scholar J. P. Moehle [1] first proposed the concept of structural seismic design thought based on structure displacement but did not use abundant building big data. This article introduces the open source distributed and storage features of the Hadoop architecture cloud platform as a subproject of the Apache Nutch project. The Hadoop cloud platform features high scalability, high fault tolerance, and flexible deployment. The storage platform is secure, stable, and reliable. MapReduce distributed computing is one of the core components of the Hadoop platform. It was first introduced by Google. It is a model and framework for

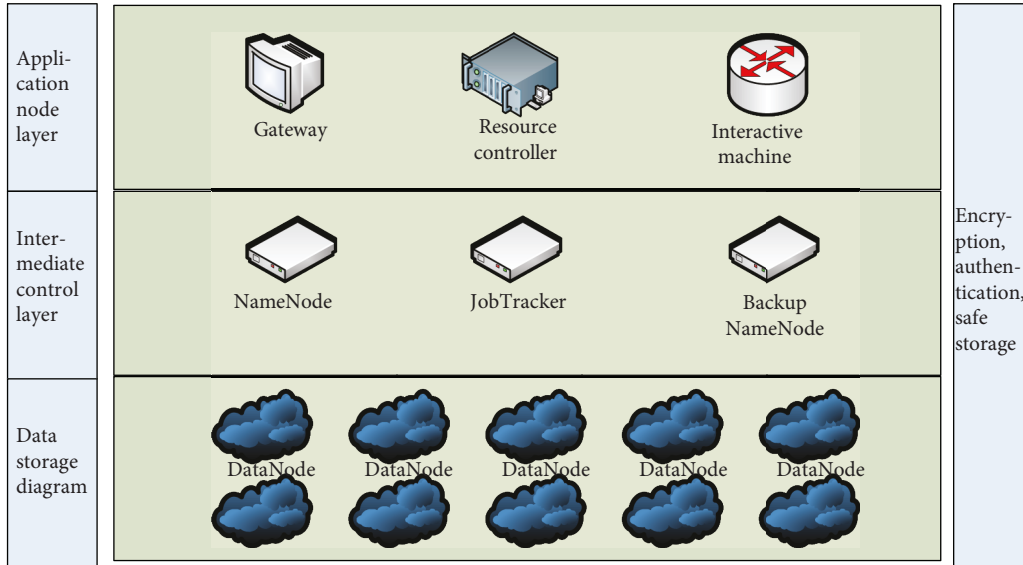


FIGURE 1: Cloud platform system based on Hadoop architecture.

computing task processing in the context of big data [2]. MapReducer's design ideas can be divided into three levels:

- (1) First of all, the parallel computing concept is adopted to divide large-scale and massive data into multiple small data blocks, which is independent of other data blocks, and uses the same calculation method to perform parallel processing on the resources, and finally, the combined results are processed
- (2) The unified system architecture is used to hide the implementation details of the system, so that programmers do not have to care about distributed details to use the platform for algorithm processing and improve the development efficiency. MapReduce can autonomously complete the following aspects of the system's underlying aspects of processing: automatic data segmentation and storage, automatically divide computing tasks and computing resources, synchronization of the node's computing tasks and data resources, merge, load balance optimization of the overall system performance, detect all nodes in the system, and handle the failure
- (3) The model abstraction of distributed computing is mainly divided into map and reduce. MapReduce draws on the ideas in the Lisp functional language; Lisp defines the overall operation of the list elements and provides similar map and reduce operations. The map and reduce functions provide an abstract parallel programming interface for the system, which can quickly parallelize the data [3]. MapReduce abstracts computational processing into two operations map and reduce. The map operation is responsible for recording and repeating calculations on a group of data. The reduce operation is responsible for further integrated

calculation and output of the calculation results of the map operation. It provides an open source computing platform for the data of reinforced concrete structures in building big data and realizes the efficient evaluation of reinforced concrete structures in building

2. Hadoop Dynamic Evaluation System for Seismic Performance

2.1. Hadoop Architecture. In general, the typical Hadoop architecture cloud platform is assumed to operate in a trusted environment. The typical Hadoop architecture cloud platform includes Hadoop cluster core nodes and auxiliary terminal interfaces. The cluster core nodes include: NameNode, backup NameNode, DataNode, and JobTracker members [4]. Therefore, the architecture of the Hadoop-based cloud platform is divided into three layers: the data storage layer, the middleware control layer, and the application node layer, as shown in Figure 1.

Among them, DataNode is the storage resource and computing resource of the Hadoop architecture cloud platform. Its main role is to store distributed system data and perform map-reduce tasks. Hadoop architecture cloud platform data information is stored on the DataNode terminal device. When the cloud platform receives a MapReduce job task, the NameNode node allocates the storage or computational resources of the current DataNode node through the resource scheduling policy, depending on the current task completion. For Hadoop-based cloud platforms with distributed file systems, the JobTracker plays a central role in controlling the NameNode node. It is responsible for submitting user tasks to the service running on each DataNode node of the TaskTracker, so this node also plays the role of resource application (please see Table 1).

TABLE 1: Performance of aseismatic building.

The earthquake levels	Performance of aseismatic building			
	I	II	III	IV
Frequent earthquake (the probability of exceeding in T years: 63%)	It basically works	Full operation	Full operation	Full operation
Seismic fortification earthquake (the probability of exceeding in T years: 10%)	Life safety	It basically works	Run	Full operation
Rare earthquake (the probability of exceeding in T years: 5%)	Close to collapse	Life safety	It basically works	Run

2.2. *HDFS Distributed File System.* HDFS is fundamental to the unified management of stored data in distributed computing. Its features such as good fault tolerance, high reliability, high availability, high throughput, and strong expansion capability provide reliable storage protection for extracting information from a vast array of data. It has brought a lot of convenience to the research and excavation processing of massive data collection (please see Figure 2). HDFS is mainly designed to solve the following problems:

- (1) *Inevitable System Errors.* People equip the Hadoop distributed file system with a file system that can be executed on general hardware conditions. Therefore, in the course of daily use, mistakes are commonplace. Hadoop distributed file system is usually composed of hundreds of server nodes. Each node stores part of the information in all databases, and any part of this system has the probability that errors will occur at any time. Therefore, fault monitoring and rapid active restart are the main building concepts of the Hadoop distributed file system
- (2) *Streaming Data Access.* Programs executed on Hadoop distributed file systems are usually not acquired on a one-time basis but are often obtained gradually, in batches. Therefore, HDFS must support high throughput of data to better serve streaming data access
- (3) *Mass Data Mining.* With the rapid increase in the amount of data, the data to be processed is usually at or above the GB level. Therefore, a distributed file system needs to be able to provide a function of saving large files and can give a substantially higher amount of data for data transfer, which can be increased to hundreds of nodes in one cluster. Any distributed file system should be able to carry large-scale file resources. Because the process of excavating large amounts of data determines when the amount of data is very large, moving the execution process to copy it is much cheaper than migrating the data that will be analyzed. When the amount of information is very large, the effect becomes more pronounced. The overhead of migrating data is greater than the cost of the mobile computing process. This can reduce the possibility of network congestion and increase the throughput of the entire platform. In other words, it is a relatively good choice to move the calculation to the vicinity of the data, which is better than moving the data to

the program execution place. Hadoop distributed file system gives the corresponding interface, so that the application can be actively moved to the data storage location to run

2.3. *MapReduce Distributed Computing Model.* MapReduce distributed computing is one of the core components of the Hadoop platform. It was first introduced by Google. It is a model and a framework for computing task processing in the context of big data [5]. MapReduce has changed the organization of large-scale computing and realized large-scale model abstraction of computing at the level of large-scale server clusters.

Similar to HDFS, MapReducer's architecture is also the most commonly used master-slave structure. This master-slave architecture makes the system more scalable and robust. Introduce MapReducer's architecture from four aspects: Job Tracker, Task Tracker, Task, and Client:

- (1) *Job Tracker.* The main track of the progress of all jobs in the system, the use of resources in the MapReduce, and the operating information submitted to the Task Scheduler. Tasks submitted to the system will be assigned to the Task Tracker to execute the corresponding job and resources and to monitor and maintain the job's operation status. The failed job will be assigned to other Task Tracker for execution at any time
- (2) *Task Tracker.* Task Tracker is mainly responsible for job tasks allocated by Job Tracker; through the monitoring of local node resources, resources are allocated to different tasks according to usage. At the same time, Task Tracker communicates with the Job Tracker through Heart Beat timing, returns information to the Job Tracker, and accepts Job Tracker's task scheduling
- (3) *Task.* Task is a specific calculation task, including Map Task and Reduce Task. The Map Task mainly refers to the processing in the map stage. The input file is parsed into <key, value> key-value pairs, and the key-value pairs are sorted and merged. The result is stored to the local disk and is partitioned by the partition function. The corresponding Reduce Task refers to the processing operation in the reduce stage, sorting the intermediate results after map processing and processing the Reduce function to generate a new <key, value> key-value pair and storing it in HDFS

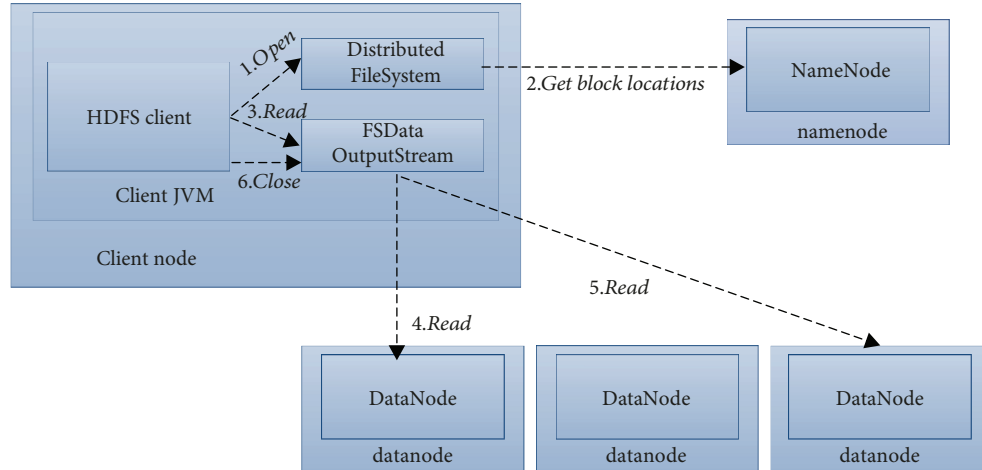


FIGURE 2: Reading process.

(4) Client. The client is used to interactively communicate with the MapReduce computing model. The user submits the task request through the client. The client submits the requested job to the Job Tracker. At the same time, the user can also view the running status of the task through the client

3. Evaluation Rules for Seismic Performance of New-Build Reinforced Concrete Frame Structures

3.1. Seismic Capacity Division of Building Structure

3.1.1. The Meaning of Earthquake Resistance. According to the theory of structural strength and ductility, the building structure resists earthquakes with its strength and ductility. When the earthquake occurs, the building structure is first resisted by the strength, the acceleration of the ground surface increases to make it yields, and then the ductility is used to resist the acceleration of the ground motion [6]. When the ductility is exhausted, the building structure will be destroyed. At this time, the acceleration of ground motion that causes structural damage is defined as the seismic capacity A_c of the building. Therefore, in the evaluation of the seismic capability of reinforced concrete frame structures, the strength and ductility of the reinforced concrete frame structure are calculated according to the size of the actual structure of the building structure and the reinforcement, combined with the internal forces of the rod components obtained by the elastic seismic analysis of the frame. Calculate the seismic capacity of the upper and lower layers of each floor of a building structure, that is, the acceleration of ground motion sustained during the destruction A_c .

3.1.2. Evaluation of Earthquake Resistance. In China's newly published "General Principles of Design for Seismic Performance of Construction Projects (Applicable)" (CECS160:2004) according to the function of the building, the buildings are divided into the following four categories [7]:

- (1) IV class: use buildings that cannot interrupt or store large quantities of dangerous or toxic substances during or after an earthquake. Once the earthquake has caused the release and alienation of these items (such as toxic gases, explosives, and radioactive materials), it will cause unacceptable harm to the public
- (2) III class: postearthquake use of buildings or densely populated construction sites where functions must be restored in the short term or are critical for post-earthquake operations, such as hospitals, schools, fire stations, police stations, communication centers, emergency control centers, and disaster relief centers
- (3) II class: all buildings and facilities except types IV, III, and I belong to this category
- (4) I class: when destroying construction earthquakes that do not endanger human life and do not cause serious property damage, such as general warehouses

3.2. Structural Failure Mode and Ductility Ratio Analysis. According to the material property and section size of the element, the strength of the structural element can be calculated according to the design code of concrete structure. However, the test results show that the bearing capacity of the element under repeated loading is lower than that under monotonic loading. Therefore, the bearing capacity of the beam and column elements calculated in this section should be multiplied by the corresponding reduction factor, where the reduction factor is 0.8 [8–10].

3.2.1. Moment Strength at the Yield of Beams and Columns. The column section bears axial force and bending moment at the same time. In the known conditions of column section size and reinforcement, the axial force-bending relation diagram (curve) is known, as shown in Figure 3. When the point corresponding to the internal force (M, P) of the column unit falls within the $M-P$ curve, the unit will not be destroyed. When the column element's internal force (M, P) is at any point on the curve, the element breaks.

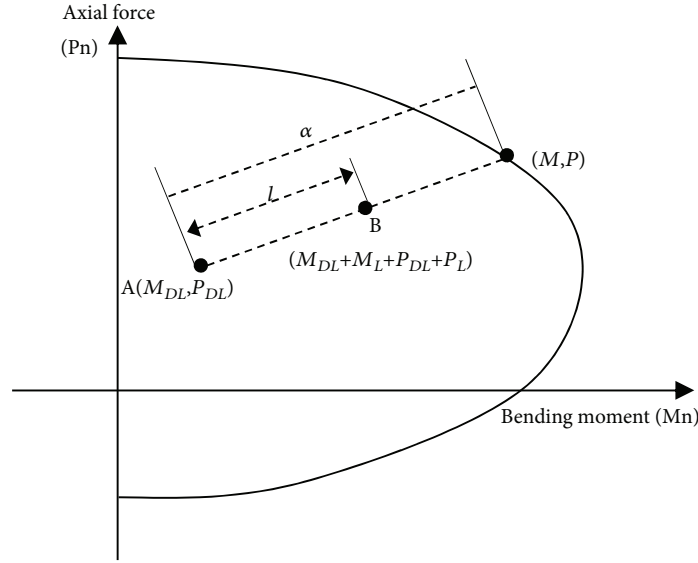


FIGURE 3: Axial force-bending moment diagram.

However, under the specific earthquake action, the failure of the unit should correspond to a certain point on a curve.

It can be seen from Figure 3 that under the action of the gravity load representative values, the generated axial force and bending moment are represented by P_{DL} and M_{DL} , respectively. Under small earthquakes (corresponding earthquake acceleration is A_g), the axial force and bending moment generated in the column section are expressed by P_E and M_E , respectively. It is assumed that when the earthquake is getting larger, the total axial force and total bending moment increase slowly along the straight line AB. When the ground motion acceleration reaches, the axial force and bending moment just intersect with the axial force and one bending moment (N - M) intensity map at point C, assuming that point C is the point where the unit failure is affected by the earthquake. At this time, the column section yields and the bending bearing capacity is $M_{DL} + \alpha M_E$. Because the axial force of the beam is very small, its axial force is set to zero.

The flexural bearing capacity of beam elements is calculated according to the "Code for Design of Concrete Structures" (GB50010-2002) [9]. The load-bearing capacity of the column section is assumed to maintain the plane according to the section strain, and the stress-strain relationship between the steel and concrete specified in the concrete specification is used for calculation.

From Figure 4, the axial equilibrium equations are listed, i.e., $\sum X = 0$. In the available form, the sum of the moments of the center point and the external force of the section is equal to zero, i.e., $\sum M = 0$, available formula is given as follows:

$$\begin{aligned} P_n &= \alpha_1 f_c b x + A'_s f'_y - \delta_s A_s, \\ M_n &= \alpha_1 f_c b x \frac{(h-x)}{2} + A'_s f'_y \frac{(h_0 - a_s)}{2} \\ &\quad - \delta_s A_s \frac{(h_0 - a_s)}{2}. \end{aligned} \quad (1)$$

In the formula, P_n is the column axial force at the time of destruction, M_n is the bending moment of the column at the time of destruction, x is the height of concrete under pressure, $A'_s f'_y$ is the area of the pressed steel bar and the yield stress, $\delta_s A_s$ is tensile stress and area of tensile reinforcement, a_s is the thickness of the concrete protective layer, $\alpha_1 f_c$ is the concrete compressive stress, h_0 is the effective height of the column section, $h_0 = h - a_s$, and h is the height of the concrete column section.

3.2.2. Shear Strength of Beam and Column Sections. The shear capacity V_n of beam and column sections is generally considered to be provided by concrete and shear reinforcement V_s . In the plastic hinge area, due to the repeated stress, the cracking of the concrete is very serious, so the part decreases with the increase of the ductility ratio. In addition, V_c is also related to the existence of axial compressive stress. If the axial compressive stress is large, V_c is effective. When the axial compressive stress is less than $0.05 f'_c$, V_c can be regarded as zero. V_n turns out to be $V_c + V_s$. When the ductility ratio reaches the ductile capacity, it is reduced to $\alpha V_c + V_s$. The value of α is calculated as follows:

$$\alpha = \begin{cases} 1.0, & P_y > 0.1 f_c A, \\ \frac{P_y - 0.05 f_c A}{0.05 f_c A}, & 0.05 f_c A \leq P_y \leq 0.1 f_c A, \\ 0, & P_y < 0.05 f_c A, \end{cases} \quad (2)$$

where A is the full cross-sectional area and P_y is the axial force at which the section yields. Under the repeated action of the ground motion, the column unit may be stressed at a certain moment and may be pulled at another time, especially for the upper column unit of the structure. In order to reduce the influence of uncertainties, only the influence of the axial force of the column element on the shear capacity of the structure under the action of the gravity load representative

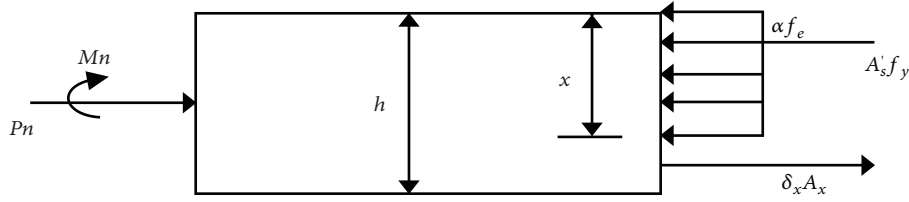


FIGURE 4: Calculation of the load-bearing capacity of column sections.

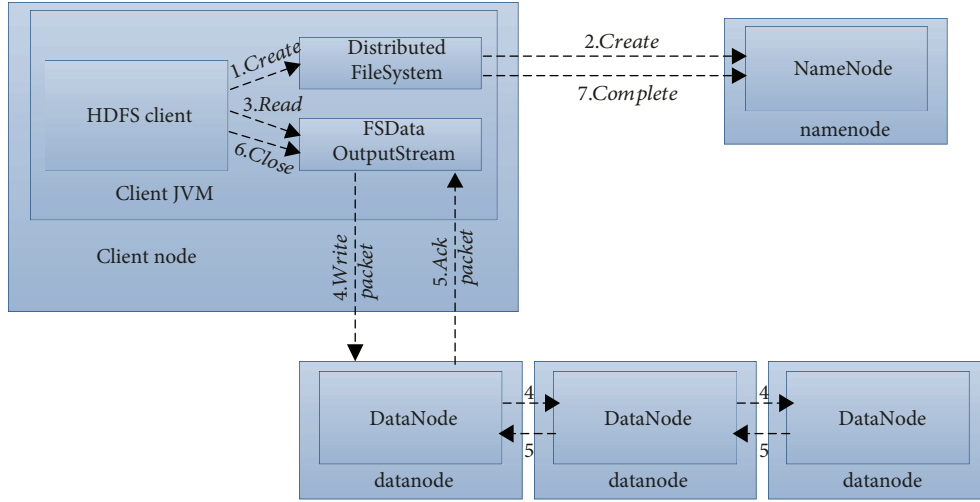


FIGURE 5: Write flow diagram.

value is considered. For ease of analysis, separate formulas for the shear capacity of beams and columns in the code are written separately. That is, V_c represents the contribution of concrete to shear capacity and V_s represents the contribution of reinforcing steel to shear capacity. Combined with the “Code for Design of Concrete Structures” (GB50010-2002) [10], the formulas for rectangular beams and columns V_c and V_s are as follows.

(1) For beams

$$\begin{aligned} V_c &= 0.7f_tbh_0, \\ V_s &= 1.25\frac{A_{sv}f_{yv}}{s}h_0 + 0.8A_{sb}f_y \sin \alpha_s. \end{aligned} \quad (3)$$

For beams that are subjected to concentrated loads (including the case where there are multiple loads in which the concentrated load is greater than 75% of the total shear value due to the shear force at the support section or the edge of the joint), shear bearing capacity is calculated as follows:

$$\begin{aligned} V_c &= \frac{1.75f_tbh_0}{\lambda + 1}, \\ V_s &= \frac{A_{sv}f_{yv}}{s}h_0 + 0.8A_{sb}f_y \sin \alpha_s, \end{aligned} \quad (4)$$

where f_t is the concrete compressive strength, A_{sv} is to configure the entire cross-sectional area of each stirrup in the same section, f_{yv} is the design value of stirrup tensile strength, A_{sb} is the curved rebar cross-sectional area in the same plane, α_s is the angle between the longitudinal axis of the reinforcing bar and the component, and f_y is the tensile strength of the platter.

(2) For the column

$$\begin{aligned} V_c &= \frac{1.75f_tbh_0}{\lambda + 1} + \beta * N, \\ V_s &= f_{yv}\frac{A_{sv}}{h_0}, \end{aligned} \quad (5)$$

where $\lambda = H_n/2h_0$, H_n is the column height, and N is the axial force of the column element under the gravity load representative value. When $N > 0.3f_cA$, A is the cross-sectional area of the component. When N is pulling force, $\beta = 0.07$. When N is pressure, $\beta = -0.2$.

(1) *Correction of Ductile Capacity.* When the bending moments of beams and columns are broken and if the stirrups of the plastic hinge area meet the requirements of the code, the ductile capacity when the beams break is defined $R_{code} = 5.0$. Ductile capacity at column failure $R_{code} = 3.0$.

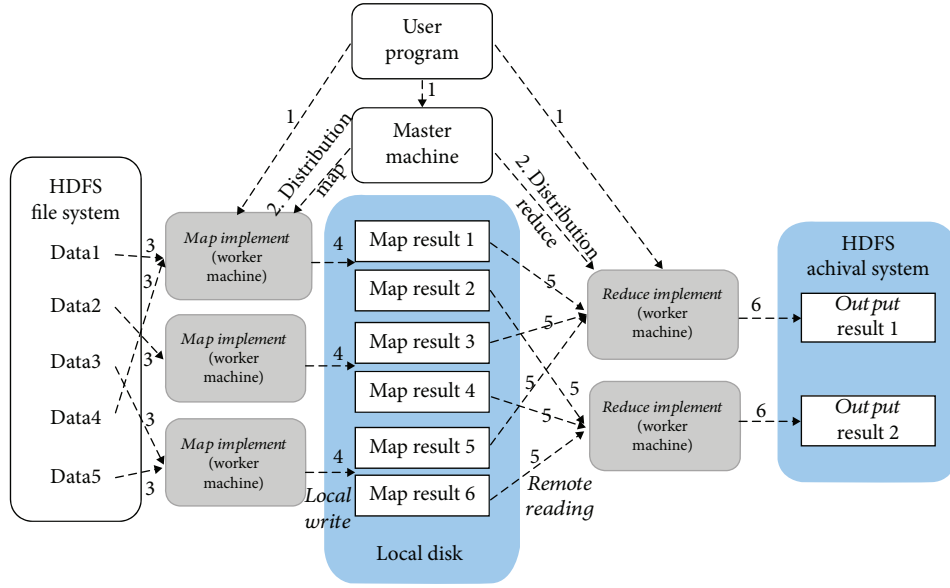


FIGURE 6: MapReduce operating mechanism diagram.

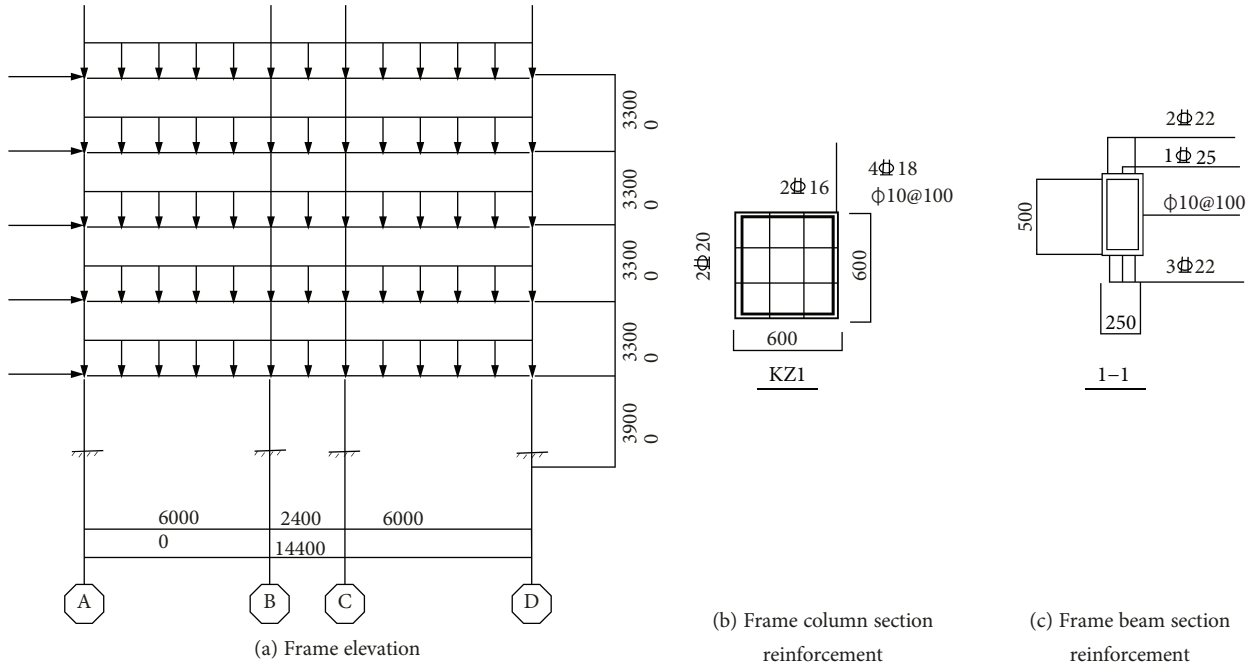


FIGURE 7: Elevation and reinforcement figure of a frame.

Otherwise, calculate the percentage of ductile reduction according to the actual constraint stirrup amount Y . At this point, the ductile capacity becomes YR_{code} , but not less than 1.0.

Y value is calculated as follows:

$$\gamma = \frac{1 + 3(1 + 5.4\alpha)(L_p/L)(2 - L_p/L)}{1 + 19.2(L_p/L)(2 - L_p/L)}, \quad (6)$$

$$\alpha = \frac{\rho_s}{\rho_{s,code}}$$

where ρ_s is reinforcement ratio, $\rho_{s,code}$ is calculated according to the "Building Seismic Design Code" (GB50011-2001) calculated by the amount of the stirrup reinforcement ratio, L_p is a plastic hinge length, $L_p = 0.08L + 6d_s$, L is the length of the joint from the bending point to the beam column, and d_b is the diameter of the main bar.

(2) Determines the Failure Mode and Ductility Ratio of Single Beam and Column. There are three failure modes for beams and columns. The first situation is shear failure. In the

TABLE 2: Reinforcement information of sections.

Section number	Section width (mm)	Section height (mm)	Stirrup diameter (mm)	Stirrup spacing (mm)	Protective layer thickness (mm)	Stirrups number of limbs	Volumetric hoop rate	Reinforcement rate
KZ1	750	750	10	100	20	5	1.08	0.52
KZ2	750	700	10	100	20	5	1.15	0.56
...
KL4	300	600	10	100	20	4	1.66	1.05

TABLE 3: Structural deterioration parameter.

Unit number	Rebar corrosion rate η_s	Rebar corrosion position correction factor k_{cr}	Environmental correction factor k_{ce}	Carbonization parameters Δc_k
10101	0.0082	0.021	0.00092	0.24
10201	0.0073	0.034	0.00098	0.37
10301	0.0072	0.029	0.0015	0.29
10401	0.0067	0.024	0.0012	0.32
10102	0.0083	0.032	0.00091	0.34
...
120407	0.0092	0.046	0.00085	0.41

second case, the shear failure occurs before the ductile capacity YR_{code} is reached although the yield of the bending moment occurs. The third situation is the destruction of ductile capacity reaching YR_{code} , and at this time no shear failure has occurred.

In the first case, the rod end bending moment is $M_{DL} + a_y M_E$. Since the yield has not yet occurred, the ductility ratio is taken as 1.0. In the second failure situation, the bending moment yield occurs, but before the ductile capacity YR_{code} is reached, the shear failure occurs and the ductility ratio is corresponding. In this case, the beam and column bear the shear force: $(1 + 0.3(R_f - 1)/(R_{code} - 1))V_y$. Its size is V_{DL} plus a certain multiple of V_E . The corresponding rod end bending moment is M_{DL} plus this multiple times M_E . In the third case, the ductile capacity has been fully used, so the ductility ratio is YR_{code} .

3.2.3. Nodal Strength Comparison, Column Bearing Shear, and Ductility. At the node where the beam and column intersect, whether the column is destroyed first or the beam first destroyed depends on the respective bending moments of the beam and column. If FB_i is greater than FC_i , it belongs to weak column strong beam. When calculating the seismic resistance of the upper or lower half of the node, the shearing force at the failure of the column is equal to the shear force at the failure of the column above, and the ductility ratio is also based on the ductility ratio obtained in the above section. If FB_i is less than FC_i , it is a strong beam. When calculating the seismic

resistance of the half-layer of the node, under the shear force assumed when the column breaks:

$$\begin{aligned} V_{ft}^{(a)} &= V_{DLi}^{(a)} + V_{CEi}^{(a)} \cdot FB_i, \\ V_{ft}^{(b)} &= V_{DLi}^{(b)} + V_{CEi}^{(b)} \cdot FB_i, \end{aligned} \quad (7)$$

where a is above the node, b is below the node, V_{DLi} is the shear force of the column under the gravity load representative value, and V_{CEi} is the shear force of the column caused by small earthquakes. The ductility ratios corresponding to the upper and lower columns of the node are calculated by weighting the ductility ratios of the left and right beams, and the moments of the earthquakes assumed when the beam is destroyed are weighted. The corresponding ductility ratios for the upper and lower columns are calculated as follows:

$$R_{fi} = R_{fi}^{(a)} = R_{fi}^{(b)} = \frac{R_{Li}(M_{fLi} - M_{DLLi}) + R_{Ri}(M_{fRi} - M_{DLRi})}{(M_{fLi} - M_{DLLi}) + (M_{fRi} - M_{DLRi})}, \quad (8)$$

where M_{fLi} and M_{fRi} are the bending moment when the left and right beams break, respectively, M_{DLLi} and M_{DLRi} are the bending moment of the left and right beams caused by the gravity load representative value, respectively, and R_{Li} and R_{Ri} are the ductility ratio of the left and right beams, respectively.

3.2.4. Acceleration of the Yielding Ground Motion of Each Half Layer. The acceleration of the yielding ground motion of each half layer is a_{yi} times the seismic acceleration corresponding to the small shock Ag . The coefficients corresponding to the upper and lower halves of the i -th layer $a_{yi}^{(a)}$ and $a_{yi}^{(b)}$ can be calculated as follows:

$$\begin{aligned} a_{yi}^{(a)} &= \frac{\sum (V_{fi}^{(a)} - V_{DLi}^{(a)})}{\sum V_{CEi}^{(a)}}, \\ a_{yi}^{(b)} &= \frac{\sum (V_{fi}^{(b)} - V_{DLi}^{(b)})}{\sum V_{CEi}^{(b)}}. \end{aligned} \quad (9)$$

In the formula, $V_{CEi}^{(a)}$ and $V_{CEi}^{(b)}$ are the shear force of the upper and lower columns of a node under the action of small

earthquakes, respectively, $V_{fi}^{(a)}$ and $V_{fi}^{(b)}$ are the shear force taken on the failure of the upper and lower columns of the node, respectively, and $V_{DLi}^{(a)}$ and $V_{DLi}^{(b)}$ are the shear force of the upper and lower columns under the action of the representative value of gravity load, respectively.

3.2.5. Seismic Reduction Coefficient in the Structural System. Seismic reduction coefficient (F_u) is the multiplier of seismic acceleration which can be increased when the structure is yielding. The ductility ratio of the system reaches the permissible ductility capacity (R_a) at this time. F_u is related to the cycle of building structure, the type of site, and the R_a . The relationship between the permissible ductility capacity (R_a) and the ductility capacity (R) is $R_a = 1 + 0.5(R - 1)$. Combined with the code for seismic design of buildings, F_u can be calculated as follows:

$$F_u = \begin{cases} R_a, & T \geq T_g, \\ \sqrt{2R_a - 1} + (R_a - \sqrt{2R_a - 1}) \left(\frac{T - ((T_g - 0.1)/2) - 0.1}{(T_g - 0.1)/2} \right), & 0.1 + \frac{(T_g - 0.1)}{2} \leq T \leq T_g, \\ \sqrt{2R_a - 1}, & 0.1 \leq T \leq 0.1 + \frac{(T_g - 0.1)}{2}, \\ \sqrt{2R_a - 1} + (\sqrt{2R_a - 1} - 1) \left(\frac{T - 0.1}{0.08} \right), & 0.02 \leq T \leq 0.1, \\ 1.0, & T \leq 0.02. \end{cases} \quad (10)$$

In the formula, T_g is a characteristic cycle (s) and T is the cycle of building structure (s). When $R_a = 1.0$, the upper computing F_u is 1.

3.2.6. Yield Ground Motion Acceleration and Seismic Capacity of Half Stories in Frame Structures. The ground acceleration of the upper and lower layers of the i layer is $a_{yi}^{(a)}$ and $a_{yi}^{(b)}$ multiplied by the seismic acceleration corresponding to the small earthquake [11–13]. The ductility capacity of the upper and lower half of the i node must be the weighted average of the ductility capacity corresponding to the failure of each node. It can be calculated as follows:

$$\begin{aligned} R_i^{(a)} &= \frac{\sum R_{Fi}^{(a)} (V_{Fi}^{(a)} - V_{DLi}^{(a)})}{\sum (V_{Ei}^{(a)} - V_{DLi}^{(a)})}, \\ R_i^{(b)} &= \frac{\sum R_{Fi}^{(b)} (V_{Fi}^{(b)} - V_{DLi}^{(b)})}{\sum (V_{Ei}^{(b)} - V_{DLi}^{(b)})}. \end{aligned} \quad (11)$$

In addition, the allowable ductility capacity of each half layer can be calculated as follows:

$$\begin{aligned} R_{ai}^{(a)} &= 1 + \frac{(R_i^{(a)} - 1)}{2}, \\ R_{ai}^{(b)} &= 1 + \frac{(R_i^{(b)} - 1)}{2}. \end{aligned} \quad (12)$$

With allowable ductility capacity, the seismic reduction factor $F_{ui}^{(a)}$ and $F_{ui}^{(b)}$ of the structural system can be calculated according to the period T and site type of the building structure.

The seismic capacity $A_{ci}^{(a)}$ and $A_{ci}^{(b)}$ of the upper and lower floors of the i level nodes can be calculated as follows:

$$\begin{aligned} A_{ci}^{(a)} &= Ag * a_{yi}^{(a)} * F_{ui}^{(a)} = A_{yi}^{(a)} F_{ui}^{(a)}, \\ A_{ci}^{(b)} &= Ag * a_{yi}^{(b)} * F_{ui}^{(b)} = A_{yi}^{(b)} F_{ui}^{(b)}. \end{aligned} \quad (13)$$

In the formula, $A_{yi}^{(a)}$ and $A_{yi}^{(b)}$ are the yield ground motion acceleration of the upper and lower half of the i node, respectively. The values of aseismic capacity for each half story may be different. For safety consideration, the minimum value of all values is taken as the aseismic capacity of the whole

building structure. Up to now, the aseismic capacity of the frame structure has been obtained.

4. Dynamic Evaluation of Seismic Performance of Reinforced Concrete Frame Structures at Present

The performance of building reinforced concrete frame structure deteriorates gradually with time or earthquake damage [14]. First, the constitutive relation of the material deterioration, the corrosion rate-based constitutive relation of reinforcement, and the slip constitutive relation considering the corrosion of the reinforced concrete are introduced. Then, it is embedded in the seismic capacity model of reinforced concrete frame structure, and a dynamic evaluation model for seismic performance is established.

4.1. Deterioration Model of Reinforced Concrete Frame Structure

4.1.1. The Constitutive Relation of Steel Deterioration Based on the Corrosion Rate. It is shown that after the corrosion of the reinforced concrete, the mechanical properties of the reinforced concrete structure will decrease sharply and the damaged form of the corroded reinforced concrete structure has obvious brittleness characteristics, especially the reinforced concrete structure which has been damaged by the earthquake [15–19]. The concrete protection layer caused by structural damage is cracked or exfoliated, which makes the reinforced bar contacts with the external environment, which greatly increases the probability of corrosion of the structure during the service period of the service. Therefore, the constitutive relationship of reinforced bars should be newly determined for seismic evaluation of deteriorated reinforced concrete structures [20]. By studying the corrosion test of a group of reinforced concrete beams, Yingshu et al. gave the constitutive relation of corroded steel bars, as shown in formula (14)–(16) and assumed that the elastic modulus of steel bars remained unchanged before and after the corrosion.

When $\eta_s \leq 5\%$,

$$\sigma'_y = (1 - 1.608\eta_s)\sigma_y, \quad (14)$$

$$\sigma' = (1 - 2.480\eta_s)\delta, \quad (15)$$

$$\xi'_u = (1 - 2.480\eta_s)\xi_u. \quad (16)$$

When $\eta_s > 5\%$,

$$\sigma'_y = (0.962 - 0.848\eta_s)\sigma_y, \quad (17)$$

$$\sigma' = (1.088 - 3.573\eta_s)\delta, \quad (18)$$

$$\xi'_u = (1.088 - 3.573\eta_s)\xi_u. \quad (19)$$

In the formula, η_s is the corrosion rate of steel, σ'_y is the yield strength of corroded steel bar, δ' is the elongation rate of corroded steel, ξ'_u is the ultimate strain of corroded steel

bar, σ_y is the yield strength of not corroded steel bar, δ is the elongation of not corroded steel bar, and ξ_u is the ultimate strain of noncorroded steel bar.

By observing the formula (17) and (18), in order to determine the constitutive relation of corroded steel bars, first, it is necessary to determine the corrosion rate of the steel bar (η_s) and the corrosion rate can be expressed by the depth of corrosion of the steel bar ($\delta(t)$). Jin Weiliang's formula for calculating the amount of steel corrosion in the literature is given as follows:

$$\delta(t) = 46 \cdot k_{cr} \cdot k_{ce} \cdot e^{0.04T} \cdot (RH - 0.45)^{2/3} \cdot c^{-1.36} f_{cu}^{-1.83} (t - t_i). \quad (20)$$

In the formula, $\delta(t)$ is the corrosion depth of steel bar and k_{cr} and k_{ce} are, respectively, the corrosion sites of reinforcement and the environmental correction factors of reinforced concrete structural members. T and RH are the annual average temperature ($^{\circ}\text{C}$) and annual average humidity (%) near the surface of reinforced concrete structures, respectively. c is the thickness of the concrete protective layer (mm), f_{cu} is the compressive strength of concrete cubes (MPa), and t and t_i are, respectively, the service life of the reinforced concrete structure and the time when the steel bar starts to rust. The initial corrosion time of reinforcement in reinforced concrete structural members can be determined by the deterioration criterion expressed as follows:

$$f(t_i) = c - \Delta c_k - x(t_i) = 0. \quad (21)$$

In the formula, Δc_k is a carbonization parameter (mm) and it is a random variable [21, 22]. In order to simplify the calculation, its mean can be determined by the following formula:

$$\Delta c_k = 4.86 \cdot (-RH^2 + 1.5RH - 0.45) \cdot (c - 5) \cdot (\ln f_{cuk} - 2.30). \quad (22)$$

4.1.2. Slip Constitutive Relation of Reinforced Concrete Connections Based on the Corrosion Rate. Xu Shanhua studied the constitutive relationship between the bond stress and the slip between the reinforced concrete and the concrete, and the relationship between the bond strength and the corrosion rate of the corroded reinforced concrete members was obtained by the regression analysis of the experimental data by mathematical regression analysis [23], as shown in the following formula:

$$\tau = \beta \cdot \tau_0. \quad (23)$$

In the formula, τ_0 is the bond strength between concrete and steel bar for noncorroded reinforced concrete members and β is the reduction coefficient of the bond

strength of corroded reinforced concrete members, as shown in the following formula:

$$\beta = \begin{cases} 1 + 0.5625\eta_s^2 + 0.055625\eta_s^3 - 0.003\eta_s^4, \\ 2.0786\eta_s^{-1.0369}. \end{cases} \quad (24)$$

Due to the surface properties of steel bars, the bond and slip of concrete and steel bar will be greatly affected. The expression of bond strength (τ_0) is generally determined by the formula recommended in *CEB-FIP Model Code 1990: Design Code*, as shown in formula (25) and (26):

(1) Glossy steel bar

$$\tau_0 = 9.78 \times 10^2 \cdot s - 5.72 \times 10^4 \cdot s^2 + 8.53 \times 10^5 \cdot s^3. \quad (25)$$

(2) Ribbed steel bar

$$\tau_0 = (61.5 \cdot s - 693 \cdot s^2 + 3.14 \times 10^3 \cdot s^3 - 0.478 \times 10^4 \cdot s^4) \cdot f_{t,s} \cdot \sqrt{\frac{c}{d}}. \quad (26)$$

In the formula, c is the thickness of concrete protective layer (mm) and d is the diameter of steel bar (mm).

4.2. Dynamic Evaluation of Seismic Behavior of Reinforced Concrete Frame Structures

4.2.1. *Hadoop Framework of Reinforced Concrete Frame Structure.* The Apache Hadoop library is a framework that extends a single server to thousands of servers; each of which provides local computing and storage rather than hardware to achieve high availability, mainly including the following modules [24]:

- (1) Hadoop common: commonly used utilities supporting other Hadoop modules
- (2) Hadoop distributed file system (HDFS): a distributed file system that provides high-throughput access to application data
- (3) Hadoop YSRN: framework for cluster job scheduling and resource management
- (4) Hadoop MapReduce: based on the YARN system, parallel processing large data sets

4.2.2. *Construction of the HDFS File System for Aseismic Performance of Reinforced Concrete.* HDFS is a master-slave architecture. If the client wants to access HDFS, it needs to complete the interaction between Name Node and Data Node. Name Node is responsible for managing the entire file system, and multiple Data Nodes is the unit responsible for storing data. When the client needs to operate the data in the file system, it communicates with the Name Node, but

the actual reading and writing operation is done directly with the Data Nodes communication.

Name Node, the master control server, is responsible for processing the Namespace of the file system, recording the location of each file data block, and undertaking the work of coordinate and scheduling and also in charge of the changes in the Namespace. Data Node is responsible for actually storing the data needed by users. The Namespace of the distributed file system is open, so that users can store data according to the style of the file. Usually each data block occupies 64 MB, and the data stored on the HDFS is usually written only once, but it will be read many times in the later use. In general, the files stored on the Hadoop distributed file system will be divided into multiple blocks based on the size of the typical block, and each block will be divided as far as possible and stored separately in a separate Data Node. Name Node is responsible for handling all kinds of Namespace operations in the file system, such as Openfiles, Closefiles, Rename, and mapping data blocks to Data Node. Data Node is responsible for executing the I/O operation of users. According to the commands of Name Node, Create, Copy, Delete, and other actions of data blocks are carried out. If the client wants to access the file, the first step needs to get all the information of the data block address from the Name Node, obtains the specific location of the data block, and then interacts directly with the corresponding node to obtain the required data.

The most basic configuration of a Hadoop distributed file system is important, which can be summarized as running Name Node on a dedicated computer and executing Data Node on other nodes, respectively. The idea of just executing a Name Node on a machine cluster largely makes the structure of the system simpler (please see Figure 5).

In Name Node, a lot of transaction logs (Edit Log) are stored. These Edit Log save various operations and updates in the distributed file system and save Namespace with Image File, including mapping and file attribute information. Edit Log and Image File retain the local disk of the main node. Each time you start, you need to get Image File and Edit Log from the disk, then read the records in the Edit Log on the Image File, and rewrite the local new Image File, which can cut out the old Edit Log, and this process is called the checkpoint. The Hadoop distributed file system also sets up a Secondary Name Node, which helps Name Node handle Image File and Edit Log. When the Name Node starts running, the Image File and Edit Log are merged, Secondary Name Node will be copied to the temporary directory on time from Name Node, and then, it will be uploaded again. Name Node updates the Image File and processes Edit Log to control the value of Edit Log under the standard.

4.2.3. *Distributed Calculation of Seismic Performance Evaluation of MapReduce.* First, the MapReduce function splits the input file into n split shards. Each shard is split into approximately 16 to 64 megabytes. Then, the shards are parsed into key-value pairs. The entire task is based on split shards. The MapReduce distributed computing model schedules multiple job tasks for computation through the core master program. The mapper will input the split assigned

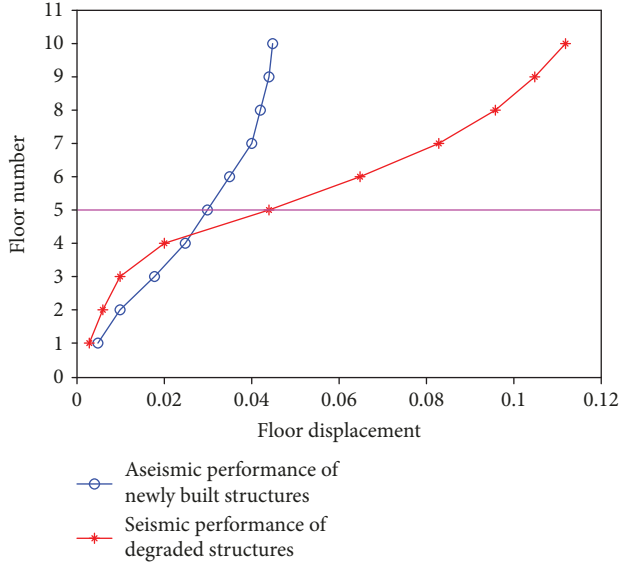


FIGURE 8: Floor displacement of different floors.

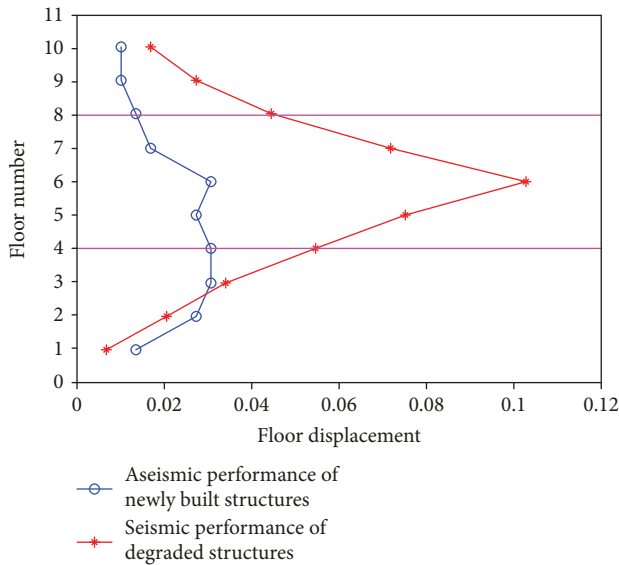


FIGURE 9: Floor displacement angle of different floors.

to it from HDFS based on the cut point of the cut. In the map phase, each split will create a corresponding map task and assign the task to the corresponding worker program. The worker program will call the map function in the system to perform the calculation and sort the intermediate results and then use the key value of the same key value. Pairs are grouped together to form a list, then the result set is divided into R partitions and stored locally. In the reduce stage, the data of different map data will be integrated. After the sort processing, a new key-value pair will be formed. Finally, the result set will be processed through the reduce function to obtain the latest result (please see Figure 6).

Finally, the output of the reduce phase will now form the output file of master and finally output to HDFS. When all

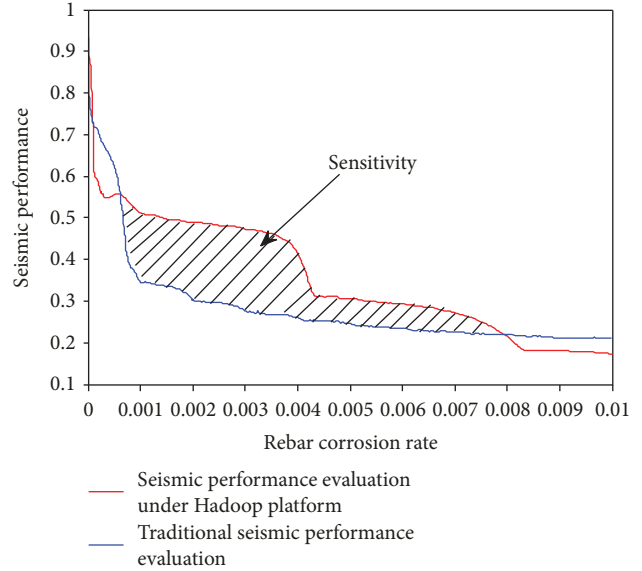


FIGURE 10: Traditional seismic performance evaluation and seismic performance evaluation under a Hadoop platform.

the map and reduce tasks of the whole process are completed, the reducer’s task will output R files, and these files can continue to be passed as input files to other MapReduce computing processes. Or these files can be invoked by other distributed system applications as resources.

5. Example Analysis

5.1. Engineering Survey. In order to systematically explain the application process of this method in seismic performance evaluation of existing reinforced concrete structures and to check its effectiveness, a project is selected in this paper: a 10-story reinforced concrete frame structure is calculated and analyzed. The project is built in 2009, class C building. In the process of analysis, a side frame is first calculated. The load arrangement and reinforcement are shown in Figure 7. The height of the 1 layer is 4.2 m, the height of the 2~10 layers is 3.6 m, and the cross section size of the frame column of the 1~3 layers is 750 mm × 750 mm; the section size of the frame column of the 4~10 layers is 700 mm × 700 mm, and the cross section of the frame beam is 300 mm × 600 mm. The standard values of the floor and live loads are 5 K and concrete, respectively, and the concrete strength grade girder and pillar takes C35; the longitudinal force bar is HRB400, and the hoop is HPB300. The concrete section hoop information is shown in Table 2, and the basic acceleration 0.20 g is designed.

In the process of building design, the reinforced concrete hoop method, that is, the material information in the hoop process, is shown in Table 2.

In order to verify the effectiveness and accuracy of the seismic performance evaluation method of this paper when the structural damage appears on different floors, the example project was built in 2009 and under normal environment to determine the degree of concrete carbonization and

reinforcement corrosion of its structure during its subsequent service life. Considering the constitutive relation of the material deterioration, the ductility curve of the members of the project is mainly determined by the stiffness and strength degradation coefficient caused by the deterioration of the structure, as shown in Table 3.

5.2. Numerical Simulation. In this paper, the framework of the reinforced concrete frame platform is constructed by using Apache Hadoop software library and the seismic performance evaluation model of the new building structure and deterioration structure data is introduced. The client has access to HDFS through the interaction between Name Node and Data Node; a write operation and multiple read operations are performed through the master control server Name Node. Then, with Hadoop as the large data processing platform, the numerical simulation of the seismic fortification intensity of 8 degrees, and the design of the basic acceleration 0.20 g, the changes in the seismic capacity of the different floors with the floor displacement and the interlayer displacement angle change, using the MapReduce function to divide into n split segments, and the output results will now form the output file of master. The final output to HDFS is shown in Figures 8–10.

From Figures 8 and 9, it is known that the corrosion of steel bar and the connection slip of reinforced concrete have great influence on the floor displacement. Floor displacement angle of the floors above 4 layers has little influence on the floor displacement angle of the top layer above 8 layers. That is, the influence of the deterioration of the reinforced concrete structure on the seismic performance of the building is mainly distributed in the 4 to 8 layers. The comparison shows that the floor displacement angle increases with the increase of floor displacement distance when the floor is below 6 stories and decreases with the increase of floor displacement distance when the floor is above 6 stories. When the deterioration structure enters the yield, the stiffness degradation is more sensitive to the damaged parts of the structure. When the number and damage degree of the structural damage component are both at the same time, the lower the location of the structural damage is, the greater the degree of the stiffness degradation after the yield of the damage structure. As shown in Figure 10, the evaluation of reinforced concrete frame structure based on Apache Hadoop software library and Hadoop for large data processing platform is compared with the traditional displacement seismic evaluation method. The Hadoop seismic assessment method under large data background has high efficiency and accuracy.

6. Conclusion

Based on the seismic performance evaluation method of structural displacement, this paper follows the idea of large data processing with distributed computing. Based on the large reinforced concrete data of high-rise buildings and the seismic performance evaluation of new buildings and existing buildings, an efficient evaluation model for seismic performance of reinforced concrete frame structures is established and the seismic characteristics of floors are analyzed.

The following conclusions can be drawn from the analysis of the seismic behavior of the floor.

- (1) Through the large data processing of reinforced concrete structure, it is found that the initial stiffness index of the structure is not sensitive to the identification of the damage location of the structure. The initial stiffness changes before and after the structural damage can only identify the seismic capacity of the structure, but cannot determine the location and size of the structural damage
- (2) The calculation results of the Hadoop seismic assessment model underestimate the interlayer displacement angle of the structure on the low floor and overestimate the interlayer displacement angle at the higher floor, but the overall error is smaller than the real value, and the smaller the upper level error is, the seismic performance evaluation results are ideal
- (3) The efficiency and accuracy of the platform based on the idea of distributed computing and big data processing can effectively improve the evaluation of RC frame structures. Efficient use of large building data improves the seismic performance evaluation method on the one hand and on the other hand improves the reliability of seismic performance evaluation results

Data Availability

The data used to support the findings of this study are available from the corresponding author upon request.

Conflicts of Interest

We declare that there is no conflict of interest regarding the publication of this paper.

References

- [1] H. He, Z. Du, W. Zhang, and A. Chen, "Optimization strategy of Hadoop small file storage for big data in healthcare," *The Journal of Supercomputing*, vol. 72, no. 10, pp. 3696–3707, 2016.
- [2] M. Kim, Y. Lee, H. H. Park, S. J. Hahn, and C. G. Lee, "Computational fluid dynamics simulation based on Hadoop ecosystem and heterogeneous computing," *Computers & Fluids*, vol. 115, pp. 1–10, 2015.
- [3] D. Shankar, X. Lu, M. Wasi-ur-Rahman, N. Islam, and D. K. Panda, "Characterizing and benchmarking stand-alone Hadoop MapReduce on modern HPC clusters," *The Journal of Supercomputing*, vol. 72, no. 12, pp. 4573–4600, 2016.
- [4] C. Li, T. Chen, Q. He, Y. Zhu, and K. Li, "MRUniNovo: an efficient tool for *de novo* peptide sequencing utilizing the Hadoop distributed computing framework," *Bioinformatics*, vol. 33, no. 6, pp. 944–946, 2016.
- [5] H. P. Wen, S. M. Yu, and L. Jin-Hu, "Encryption algorithm based on Hadoop and non-degenerate high-dimensional discrete hyperchaotic system," *Acta Physica Sinica*, vol. 66, article 230503, 2017.

- [6] M. Lupoae, C. Baciú, D. Constantin, and H. Puscau, "Aspects concerning progressive collapse of a reinforced concrete frame structure with infill walls," in *Proceedings of the World Congress on Engineering (WCE 2011)*, pp. 2198–2203, London, UK, July 2011.
- [7] H. J. Dai and Q. I. Ai, "Analysis on seismic-response of reinforced concrete frame structure with different-thickness staircase," *Journal of Fuzhou University*, vol. 39, no. 1, pp. 101–109, 2011.
- [8] A. Pavese, I. Lanese, and R. Nascimbene, "Seismic vulnerability assessment of an infilled reinforced concrete frame structure designed for gravity loads," *Journal of Earthquake Engineering*, vol. 21, no. 2, pp. 267–289, 2016.
- [9] K. Zhou, N. N. Chen, and S. Y. Chen, "Pounding analysis of the main-podium reinforced concrete frame structure based on open sees," *Earthquake Resistant Engineering & Retrofitting*, vol. 39, pp. 22–29, 2017.
- [10] T. Xiao, R. Liu, and H. Qiu, "The influence of cast-in-place slab on distribution of hysteretic dissipative energy for reinforced concrete frame structure," *Zhendong Ceshi Yu Zhenduan/journal of Vibration Measurement & Diagnosis*, vol. 37, no. 4, pp. 750–755, 2017.
- [11] X. H. Nguyen and H. C. Nguyen, "Seismic behavior of non-seismically designed reinforced concrete frame structure," *Earthquakes and Structures*, vol. 11, no. 2, pp. 281–295, 2016.
- [12] S. Li, Z. Zuo, C. Zhai, S. Xu, and L. Xie, "Shaking table test on the collapse process of a three-story reinforced concrete frame structure," *Engineering Structures*, vol. 118, pp. 156–166, 2016.
- [13] Z. D. Xu, P. P. Gai, H. Y. Zhao, X. H. Huang, and L. Y. Lu, "Experimental and theoretical study on a building structure controlled by multi-dimensional earthquake isolation and mitigation devices," *Nonlinear Dynamics*, vol. 89, pp. 723–740, 2017.
- [14] H. Fu, Z. Li, Z. Liu, and Z. Wang, "Research on big data digging of hot topics about recycled water use on micro-blog based on particle swarm optimization," *Sustainability*, vol. 10, no. 7, p. 2488, 2018.
- [15] S. Jiang, M. Lian, C. Lu, Q. Gu, S. Ruan, and X. Xie, "Ensemble prediction algorithm of anomaly monitoring based on big data analysis platform of open-pit mine slope," *Complexity*, vol. 2018, Article ID 1048756, 13 pages, 2018.
- [16] C. Li, T. Chen, Q. He, Y. Zhu, and K. Li, "MRUniNovo: an efficient tool for de novo peptide sequencing utilizing the Hadoop distributed computing framework," *Bioinformatics*, vol. 33, no. 6, p. 944, 2016.
- [17] M. D. C Ramos, G. Mosqueda, and M. J. Hashemi, "Large-scale hybrid simulation of a steel moment frame building structure through collapse," *Journal of Structural Engineering*, vol. 142, no. 1, Article ID 04015086, 2016.
- [18] A. M. Yang, X. L. Yang, J. C. Chang, B. Bai, F. B. Kong, and Q. B. Ran, "Research on a fusion scheme of cellular network and wireless sensor networks for cyber physical social systems," *IEEE Access*, vol. 6, pp. 18786–18794, 2018.
- [19] A. Almeida, R. Ferreira, J. M. Proença, and A. S. Gago, "Seismic retrofit of RC building structures with Buckling Restrained Braces," *Engineering Structures*, vol. 130, pp. 14–22, 2017.
- [20] A. Fathieh and O. Mercan, "Seismic evaluation of modular steel buildings," *Engineering Structures*, vol. 122, pp. 83–92, 2016.
- [21] W. Zhang, L. I. Chongkai, G. U. Xianglin, and H. Dai, "Stochastic model of constitutive relationship for corroded steel bars," *Journal of Building Materials*, vol. 17, pp. 920–926, 2014.
- [22] W. Zhang, G. U. Xianglin, X. Jin, and X. Jin, "Study on corrosion mechanism of steel bars in concrete and mechanical performance of corroded steel bars," *Journal of Building Structures*, vol. 31, pp. 327–332, 2010.
- [23] M. S. Islam and S. Alam, "Principal component and multiple regression analysis for steel fiber reinforced concrete (SFRC) beams," *International Journal of Concrete Structures & Materials*, vol. 7, no. 4, pp. 303–317, 2013.
- [24] G. Cattaneo, U. F. Petrillo, R. Giancarlo, and G. Roscigno, "An effective extension of the applicability of alignment-free biological sequence comparison algorithms with Hadoop," *Journal of Supercomputing*, vol. 73, no. 4, pp. 1467–1483, 2017.

